Hydrol. Earth Syst. Sci. Discuss., 10, 2549–2600, 2013
www.hydrol-earth-syst-sci-discuss.net/10/2549/2013/
doi:10.5194/hessd-10-2549-2013

Hydrology and Earth System Sciences
Discussions
Open Access

Controls on groundwater response and runoff source area dynamics in a snowmelt-dominated montane catchment

R. S. Smith[1], R. D. Moore[2], M. Weiler[3], and G. Jost[4]

[1]WaterSmith Research Inc., 450 Cadder Avenue, Kelowna, British Columbia, V1Y5N3, Canada
[2]Departments of Geography and Forest Resources Management, University of British Columbia, 1984 West Mall, Vancouver, British Columbia, V6T1Z2, Canada
[3]Faculty of Environment and Natural Resources, University of Freiburg, Fahnenbergplatz, 79098 Freiburg, Germany
[4]Generation Resource Management, BC Hydro, 6911 Southpoint Drive, 9th Floor, Burnaby, British Columbia, V3N4X8, Canada

Received: 2 January 2013 – Accepted: 26 January 2013 – Published: 28 February 2013

Correspondence to: R. S. Smith (rsmith@watersmith.ca)

Published by Copernicus Publications on behalf of the European Geosciences Union.

Abstract

The role of spatial variability in water inputs on runoff source area dynamics has generally not received as much research attention as topography and soils; however, the influence of topography and forest cover on snow surface energy exchanges can result in asynchronous snowmelt throughout a catchment complicating the space-time patterns of runoff generation. This study investigates temporal variation in the relative importance of spatial controls on the occurrence, timing, and persistence of shallow groundwater response utilizing a highly distributed monitoring network in a snowmelt-dominated montane catchment in western Canada. The study findings indicate that deep soil hydraulic conductivity is a first-order control on the distribution of sites that generate shallow groundwater response versus sites that experience only deep percolation. Upslope contributing area and slope gradient are first-order controls on the persistence of groundwater response during peak flow, recession flow, and low flow periods. Runoff source areas expand and contract throughout these periods according to an interplay between catchment wetness and the spatial patterns of topographic convergence. However, controls on the differential timing, intensity, and quantity of snowmelt and controls on vertical versus lateral flux partitioning in the soil overwhelm the influence of topographic convergence on runoff source area dynamics during early spring freshet periods. The study findings suggest that various topographic indices and topography-based rainfall runoff models are not necessarily applicable to modelling snowmelt runoff source area dynamics during all streamflow periods for snowmelt-dominated montane catchments.

1 Introduction

Understanding runoff generation processes and streamflow source area dynamics is important for predicting streamflow quantity, quality, and timing, and for assessing the potential impacts of land use and climate changes on water resources (Beschta et al.,

HESSD
10, 2549–2600, 2013

2000; Stewart, 2009; Stewart et al., 2005). As a consequence, runoff generation has been a prominent research theme in hydrology for decades, with much greater focus on rainfall runoff than snowmelt runoff. For rainfall-dominated catchments, conceptual models of runoff source area dynamics have typically emphasized the influences of topography and soil characteristics on the downslope flow of water, particularly in relation to flow convergence, connectivity of hillslope flowpaths, and threshold responses (Dunne and Black, 1970a,b; Freeze, 1972; Hewlett and Hibbert, 1963, 1967; Sidle et al., 2000; Tromp-van Meerveld and McDonnell, 2006a,b; Tromp-van Meerveld et al., 2007; Penna et al., 2011; Ali et al., 2011). For example, the hydrogeomorphic concept articulated by Sidle et al. (2000) focuses on the activation of different hydrogeomorphic units as a function of catchment wetness. The *fill and spill* concept similarly examines runoff generation in relation to the effects of soil wetness on flowpath continuity (Tromp-van Meerveld and McDonnell, 2006a,b).

Most runoff in montane catchments is generated via subsurface flow, particularly through matrix or macropore flow within saturated soils, and via saturation-excess overland flow or return flow, which are dependent on soils being saturated to the surface (Buttle, 1994; Buttle et al., 2004; McGlynn et al., 1999; Sidle et al., 2000; Sklash and Farvolden, 1979). Infiltration-excess overland flow is rare in montane catchments due to generally high infiltration capacities relative to maximum water input intensities. Exceptions include disturbed sites such as logging roads and locations where soil freezing reduces the infiltration capacity due to the presence of ice-filled soil pores (Dunne and Black, 1971; Laudon et al., 2004; Stadler et al., 1996; Stein et al., 1994). At many montane sites, soils are relatively shallow, highly permeable, and are underlain by relatively impermeable bedrock or glacial till (Freer et al., 2002; Kim et al., 2004; McGlynn et al., 1999; Sidle et al., 2000). Under these conditions, saturated zones form above the confining basal layer and topographic indices have been found to be effective for predicting the spatial patterns of soil saturation, hydrologic connectivity, and runoff generation (Thompson and Moore, 1996; Beven and Kirkby, 1979; Freer et al., 2002). However, at sites with deeper soils, transient saturated zones can form within the soil at depths where the rate of downward percolation exceeds the ability of the soil's hydraulic conductivity to allow drainage, resulting in percolation-excess runoff generation (Redding and Devito, 2008, 2010).

The role of spatial variability in water inputs on runoff source area dynamics has generally not received as much attention as topography and soils, particularly at the scale of headwater catchments where much of the research on rainfall runoff processes has been conducted. While mountainous topography can significantly influence the spatial distribution of rainfall (Goodrich et al., 1995; Guan et al., 2005; Linderson, 2003; Shoji and Kitaura, 2006; Hrachowitz and Weiler, 2011), some studies indicate that the spatial variability of rainfall decreases with increasing event magnitude (Linderson, 2003; Taupin, 1997). In contrast, snowmelt inputs can exhibit significant and systematic spatial variability, even in headwater catchments, due to the influences of slope, aspect, elevation, and forest cover on both snow accumulation and snowmelt processes (Balk and Elder, 2000; Berris and Harr, 1987; Jost et al., 2007; Toews and Gluns, 1986; Winkler et al., 2005). In regions where melt is dominated by radiation, seasonal melt begins earlier and typically occurs at higher rates at sites with high insolation (e.g. south-facing sites in the Northern Hemisphere) (Toews and Gluns, 1986; Jost et al., 2007) and at sites lacking shading from forest cover (Anderton et al., 2002; Daly et al., 2000; Hock, 1999; Marks et al., 2002; Winkler et al., 2005). Where melt is dominated by the turbulent fluxes of sensible and latent heat, open sites with higher wind speeds experience higher melt rates than those with forest cover (Berris and Harr, 1987). The influence of topography and forest cover on snow surface energy exchanges can result in desynchronization of snowmelt throughout a catchment (Boyer et al., 2000; Jost et al., 2007), complicating the space-time patterns of runoff generation. Further complexity arises because some physiographic variables can exert contrasting influences on snowmelt runoff. For instance, sites with high insolation might experience more evapotranspiration throughout the growing season and more sublimation throughout the winter season resulting in drier soils and less snow prior to spring melt. However, the same sites might also experience more rapid snowmelt due to greater energy inputs and, therefore, potentially more rapid runoff response once soils are sufficiently wet. On the other hand, the influences of drier antecedent soil wetness and less snow as water input to the soil could overwhelm the influence of higher melt rates in some circumstances. Because of the differences in water input dynamics between rainfall and snowmelt processes, it cannot be assumed that the existing conceptual models of rainfall runoff (Dunne and Black, 1970a,b; Freeze, 1972; Hewlett and Hibbert, 1963, 1967; Sidle et al., 2000) appropriately represent runoff source area dynamics in snowmelt-dominated mountainous catchments. In particular, topographic and geologic controls on flowpath convergence and hydrologic connectivity might be of lower importance than meteorological controls on water input patterns in determining runoff source area dynamics during snowmelt.

Since runoff generation in forested catchments typically depends on the development of phreatic conditions within the soil, understanding groundwater (used here to refer to phreatic water regardless of the depth below the soil surface) dynamics is important for understanding runoff source area dynamics (Anderson and Burt, 1978; Jencso et al., 2009; Kuras et al., 2008; Monteith et al., 2006a,b; Seibert et al., 2003). Among studies that investigated groundwater related runoff source area dynamics in snowmelt-dominated forested catchments, most have been conducted in small catchments (e.g. 0.3–50 ha) with limited elevation ranges (e.g. 20–200 m of relief) (Buttle et al., 2004; Dunne and Black, 1971; Flerchinger and Cooley, 2000; Laudon et al., 2004; McDaniel et al., 2008; McNamara et al., 2005; Monteith et al., 2006a,b; Seibert et al., 2003), which would have limited the spatial variability in the timing, quantity, and intensity of snowmelt water inputs and associated impacts on runoff generation patterns. Larger or higher-relief catchments with complex terrain and variable land cover experience large gradients in meteorological and snowpack conditions that could generate asynchronous snowmelt, leading to isolated areas of groundwater response. Only a few studies have addressed groundwater dynamics within the context of asynchronous water inputs that can occur under snowmelt conditions (Boyer et al., 1995, 1997, 2000; Deng et al., 1994; Kuras et al., 2008) and several of these focused more on the flushing

HESSD
10, 2549–2600, 2013

of dissolved organic carbon than on runoff generation processes (Boyer et al., 1995, 1997, 2000).

The current study focuses on groundwater dynamics and their implications for runoff generation in the Cotton Creek Experimental Watershed (CCEW), a snowmelt-dominated montane catchment in southeastern British Columbia, Canada, with complex terrain and variable forest cover. Unlike many other montane study sites that have relatively shallow soils (Sidle et al., 2000; McGlynn et al., 1999; Freer et al., 2002), CCEW is mantled by deep glacial tills in excess of 8 m in some areas. It is hypothesized that, at sites like CCEW, (1) surface topography is less important in controlling runoff source area dynamics than other factors; (2) deep soil (e.g. 0.5 to 2 m depth) hydraulic conductivity is an important control on the overall occurrence of shallow groundwater response during all streamflow periods due to its influence on the partitioning of vertical versus lateral soil water fluxes, with locations having greater deep soil hydraulic conductivity experiencing deeper percolation and, thus, less shallow groundwater response; (3) the dominant controls on groundwater response differ between periods with and without active snowmelt, and the dominant controls also vary with time during each period; (4) upslope drainage area and hillslope gradient are dominant controls on the spatial distribution of groundwater response throughout non-snowmelt periods due to their influences on flowpath convergence, and they counteract each other in their influence on the persistence of groundwater response, with the former having a positive relation and the latter having a negative relation; (5) the localized influences of elevation, insolation, and vegetation on energy inputs to the snowpack overwhelm the influences of upslope drainage area and slope gradient on the spatial distribution of groundwater response during snowmelt periods; and (6) locations with greater solar radiation incident on the snow surface experience greater groundwater response during the early melt periods and locations with lower solar radiation incident on the snow surface experience greater groundwater response during later melt periods.

HESSD
10, 2549–2600, 2013

2 Methods

2.1 Study area

The study was conducted within the 3.5 km^2 Upper Elk Creek (UEC) sub-catchment (49° 21′ 28″ N and 115° 46′ 11″ W) of the CCEW near Cranbrook, British Columbia, Canada, approximately 540 km east of Vancouver (Fig. 1). This study is part of the CCEW project, which focused on the effects of forest harvesting and natural disturbance on snow accumulation and melt, runoff generation, and sediment transport (Smith, 2011; Jost et al., 2007, 2009; Szeftel et al., 2011; Szeftel, 2010; Smith et al., 2013).

The UEC catchment is 72.0 % forested with two main stand types: (1) stands dominated by subalpine fir (*Abies lasiocarpa*) and Engelmann spruce (*Picea engelmannii*), and (2) stands dominated by lodgepole pine (*Pinus contorta*) and western larch (*Larix occidentalis*). Clearcuts in early stages of regeneration and two bedrock outcrops comprise 27.5 % and 0.5 % of the catchment, respectively. Hillslope gradients within the UEC catchment average 27 %, ranging between nearly flat and 100 %, and elevations range between 1438 and 1938 m. Mean annual precipitation is approximately 780 mm at the Upper Cotton (UC) climate station, which is at 1780 m elevation and approximately 750 m south of the UEC catchment boundary. Annual evapotranspiration within forested areas of the catchment is 450–550 mm based on modelling results (Smith, 2011). Annual, January, and July air temperatures at the UC climate station average 2.3, −7.6, and 16.8 °C, respectively. Spring snowmelt dominates the hydrologic regime. Snowpacks usually persist from October or November through April, May, or June. Maximum snowpack storage throughout the catchment varies between approximately 150 mm and 600 mm of snow water equivalent (SWE) during an average snowpack year.

Soils throughout the UEC catchment are dominated by sands and silts with abundant coarse fragments. They developed primarily in deep (in excess of 8 m in some areas) morainal tills with some isolated areas of colluvium (BC Geological Survey,

HESSD
10, 2549–2600, 2013

2012). Except at a limited number of isolated ridge top outcrops, bedrock is not observed throughout most of the catchment, including along most road cuts, some of which exceed a depth of 8 m. Based on visual observations, the majority of vegetation roots reside within the upper 30 cm of soil with a lower root density between 30 cm and 50 cm below the surface. Few roots were observed below 50 cm depth, except for a small number of trees along several kilometers of new forestry road that had tap roots exceeding 1 m depth. Although soil physical properties (particularly soil texture, coarse fragment content, and porosity) vary considerably across the catchment, vertical variations are, for the most part, gradual with little distinct soil layering. Generally, soils vary gradually from low density and high permeability at the surface to higher density and lower permeability at depth; however, some sites show negligible change (both visible and measured) in structure, texture, or permeability with depth to at least 1.5 m. By volume, soils sampled at 45–55 cm depth average 42 % porosity, 3 % organics, 17 % sand, 19 % silt, 2 % clay, and 17 % coarse fragments, based on the USDA soil classification system (Smith, 2011). Large inter-connected soil macropores or cracks were generally not observed, likely due to the limited amount of lateral vegetation roots below 30 cm depth, the absence or limited abundance (based on visual observations) of burrowing animals (e.g. small mammals, earthworms) in the catchment, and the low clay content of the soils. The only exceptions were at the heads of ephemeral streams where large inter-connected macropores were observed that had likely developed via subsurface erosional processes.

2.2 Study design and field measurements

Fifty hillslope monitoring sites were established (33 in October 2005 and 17 in July 2006) at stratified random locations throughout the UEC catchment (Fig. 1). Stratified random sampling was used to minimize the potential for investigator bias in site selection, and to ensure that statistical inferences could be reliably extrapolated to the entire study catchment. The sample size was selected to maximize statistical power while ensuring the infrastructure could be maintained by one person, particularly during

HESSD
10, 2549–2600, 2013

installation and snow sampling. Strata were defined based on elevation (50 % of the sites were established at locations above and 50 % below the mean catchment elevation), insolation (50 % of the sites at locations greater than and 50 % less than the mean annual potential solar radiation within the catchment), forest cover (25 % of the sites in clearcuts or regenerating stands and 75 % in forested areas), and hydrogeomorphic position (20 % of the sites in each of the following classes: riparian, concave-wet, concave-dry, convex-wet, and convex-dry). For the hydrogeomorphic classes, riparian was defined as being located within 10 m of the catchment or sub-basin main-stem channels. Concave versus convex was defined as positive and negative values, respectively, of the Laplacian operator computed from a 3 × 3 neighborhood of cells surrounding each cell of interest in a 25 m resolution digital elevation model (DEM) obtained from the BC Ministry of Forests, Land and Natural Resource Operations. Wet versus dry was defined as a topographic wetness index greater than and less than the catchment mean, respectively. Elevation, insolation, and forest cover were selected for catchment stratification because they strongly influence snow depth, timing and intensity of melt, amount of evapotranspiration, and soil wetness. Hydrogeomorphic position was selected because of its association with subsurface runoff processes via flowpath convergence and divergence. The term *hillslope hollow* is used hereafter to refer to areas of pronounced surface concavity. The DEM analyses were conducted using Rivertools 3.0 (Rivix LLC, 2012). Potential solar radiation was modelled using Solar Analyst in ArcGIS 9.3.1 (ESRI, 2012).

At each site, groundwater wells were manually installed to the greatest depth possible, with the maximum depths limited by the abundance of large cobbles and boulders. Wells were selected rather than piezometers in order to capture the timing of groundwater initiation and subsequent water table dynamics rather than capturing only hydraulic head at a specific depth in the soil. For the initial installation, PVC wells with a 3.8 cm inside diameter were installed in soil pits that were dug by hand using augers, shovels, picks, and pry-bars. They were screened by cutting narrow slits in the sidewalls with 2 to 3 cm spacing and wrapping the pipes with geotextile to prevent the potential

HESSD
10, 2549–2600, 2013

influx of sediments. The soil pits were back-filled with native soil. At sites with limited or no groundwater responses, up to two additional attempts were made to increase the depths of the wells to improve the chances of observing groundwater responses, including installation of stainless steel drive-point wells using a sledgehammer. The steel wells were screened with narrow slits at 2 mm spacing. Driving the steel wells into the soil inhibited wrapping them with geotextile; however, sedimentation never became an issue. After the final installations were complete, the minimum, mean, and maximum well depths were 0.50 m, 1.09 m, and 1.64 m, respectively, and the wells were screened from the well bottom up to an average depth below the soil surface of 8 cm. Water table depth at each well was recorded every 30 min using Odyssey capacitance water level recorders (0.8 mm resolution) (Dataflow Systems Pty Limited, 2012). A PVC pipe was installed within the steel wells to insulate the Odyssey sensors from potential interference. For the analyses, it is assumed that any soil disturbance that occurred during the well installation process did not affect the water table dynamics at the sites due to the relatively small area of disturbance.

Between October 2005 and September 2008, field campaigns were conducted in early February and early April, every 2 to 4 weeks from April to early June, and once each in early summer, late summer, and mid-fall. SWE and snow depth were measured manually during site visits throughout winter and spring. Soil saturation was measured year-round by manually inserting an AquaPro capacitance probe (AquaPro Sensors, 2012) to the desired depth in an epoxy access tube that had been installed in the soil during the snow-free season. PVC extension tubes were added to the epoxy access tubes for the winter period to facilitate soil saturation measurements below the snowpack. SWE was measured using a Federal snow sampler. At each hillslope site, five snow samples were spaced at 4 m intervals on a contour across the hillslope centered at 5 m upslope from the groundwater well. Additional details of the data collection infrastructure at the hillslope sites are provided in Table 1 and in Smith (2011).

At six of the 50 hillslope sites, additional automated instruments were installed in October 2006. ECH_2O sensors and Decagon loggers (Decagon Devices Inc., 2012)

HESSD
10, 2549–2600, 2013

were used to record volumetric soil water content and air temperature, as well as water input (i.e. snowmelt/rainfall) depth from snowmelt lysimeters. These six sites are referred to as *lysimeter sites*, whereas all 50 sites that monitor hillslope runoff processes (including the six lysimeter sites) are referred to as *hillslope sites*. Additional details of the data collection infrastructure and physiography at the lysimeter sites are provided in Smith (2011).

Precipitation, air temperature, incoming short-wave radiation, relative humidity, wind speed, and snow depth were obtained from two automated climate stations located in regenerating clearcuts: the UC climate station (1780 m elevation, 750 m south of the UEC catchment) and the Lower Cotton (LC) climate station (1390 m elevation, 1500 m southwest of the UEC catchment). Continuous SWE data were obtained from the British Columbia Ministry of Environment for the Moyie Mountain snow pillow (ID# 2C10P) located at 1930 m elevation and approximately 12 km south of the UEC catchment.

Soil samples (approximately 500 g dry mass) from the 45–50 cm depth at each of the 50 hillslope sites were analyzed to quantify the porosity, texture, and fractions of coarse fragment and organic matter. After burning the soil samples to remove organic matter, grain size distributions were determined using wet sieving for particles larger than 0.05 mm and a sedigraph for smaller particles. Due to the relatively small size of the soil samples, the fractions of coarse fragments are not representative of particles larger than approximately 1 cm in diameter. At two sites, multiple samples were gathered from a range of depths up to 1.1 m to assess vertical variations in soil properties. Vertical variation in soil properties at each site was also noted from field-based observations (including manual soil texture tests) made during installation of groundwater wells and soil moisture instruments.

Field saturated hydraulic conductivity (K_s) was measured using a Guelph Permeameter at approximately 0.25 m (49 sites), 0.50 m (47 sites), 0.75 m (39 sites), 1.00 m (10 sites), 1.25 m (3 sites), and 1.50 m (1 site) soil depths. The resulting K_s values were averages of vertical and horizontal conductivities since depth and width dimensions of

HESSD
10, 2549–2600, 2013

the water-filled portion of the bore-hole were approximately equal; however, hydraulic conductivity is likely to be relatively isotropic throughout the catchment since the soils are dominated by sand, silt, and gravel with minimal amounts of clay and since the soils are not stratified (Mitchell, 1993). For each measurement, a 7 cm diameter hole was augered to the desired soil depth and two K_s tests were conducted – one with 5 cm of hydraulic head and the other with 10 cm of head. K_s was calculated for each test using methods described in the Guelph Permeameter operating instructions (Soil Moisture Equipment Corp, 1991) and the arithmetic mean of both tests was used as the final K_s value.

2.3 Analysis

2.3.1 DEM development

After establishment of the hillslope sites, it became clear that the topographic variability across the hillslope (i.e. on contour) was not adequately represented by the 25 m resolution of the original DEM. Therefore, a 5 m resolution DEM was developed using photo interpretation methods applied to 1 : 15 000 scale aerial photos (LIDAR was cost prohibitive). The raw photo interpretation points were supplemented with GPS points (Trimble ProXT GPS and Ranger data logger) gathered over a minimum area of 100 m by 100 m centered over each hillslope site. The final DEM was interpolated to a 5 m resolution using triangulation and was smoothed using a Gaussian filter. R statistical software (R Development Core Team, 2010) was used for merging and filtering the raw point data. SAGA GIS (SAGA User Group Association, 2012) was used for grid averaging the point data and for interpolating and filtering the DEM. Rivertools 3.0 was used for calculating plan curvature, slope gradient, and aspect from the DEM.

HESSD
10, 2549–2600, 2013

2.3.2 Site parameters

Table 2 provides a list of site parameters that were measured or calculated to characterize each site and were used in statistical analyses to investigate the influences of site physiography on groundwater response. ArcGIS 9.3.1 (ESRI) was used for delineating and calculating the upslope drainage area (using a D8 grid) for the hillslope sites and for manually determining the elevation rise and fall to the upslope ridge and downslope channel (along the flowpath), respectively. The topographic wetness index was calculated for each site using the upslope drainage area per unit contour width of the DEM and the mean hillslope gradient from field observations. To account for the effects of site aspect and hillslope shading on energy inputs, potential solar radiation (direct and diffuse) was modeled for each day of the year for each hillslope site using ArcGIS 9.3.1 (ESRI). To incorporate the seasonal variation in potential solar radiation within statistical analyses, radiation was averaged for three seasons of the year: the snow accumulation season (November through March), the snowmelt season (April and May), and the snow-free season (June through October). Forest cover basal area was calculated for each site using the forest cover survey data. For calculating the portion of the upslope drainage area that is logged, all areas in an early stage of regeneration were grouped together.

2.3.3 Statistical analysis

The common period of record for the streamflow and groundwater datasets was limited to the period from 1 November 2007 to 20 September 2008. Notwithstanding the fact that data from late September and all of October are missing from the period of record, inference is made as though the period of record incorporates an entire year since the autumn period is hydrologically relatively inactive in the UEC catchment.

Groundwater dynamics throughout the catchment were grouped into three classes: persistent, transient, and unresponsive (i.e. no formation of a saturated layer within the observed soil profile). Groundwater responses were temporally discontinuous at most sites and detectible groundwater responses were never recorded at 13 of the 50 hillslope sites. Due to this data censoring, statistical analysis methods such as ordinary regression could not be applied without removing the sites that did not experience groundwater responses, which would have led to a substantial loss of spatial information. As a result, the analyses were based on an ordered classification of the groundwater response data and ordinal logistic regression (OLR) was applied to predict the probability of a site meeting or exceeding each ordered class using the selected site parameters (Table 2) as predictors. OLR is an extension of binary logistic regression (LR). LR forms a linear regression between the natural logarithm of the odds ratio (O) for a response variable and one or more predictor variables:

$$\ln(O) = a + \boldsymbol{b} \cdot \boldsymbol{x} \tag{1}$$

where a is a constant, $\boldsymbol{b}$ is a vector of slope coefficients, and $\boldsymbol{x}$ is a vector of predictor variables. The odds ratio for the response is the probability of being in one group divided by the probability of being in the other group,

$$O = \frac{p}{1-p} \tag{2}$$

where p is the probability of a response being in a given or higher level category. An extensive review of OLR can be found in McCullagh (1980).

The period of record was separated into eight hydrologically distinct periods to investigate whether spatial patterns of groundwater response can be linked to seasonal changes in catchment hydrologic conditions. Each period was intended to represent a distinct phase of water input (related to variability in meteorological conditions) and resulting runoff response (Fig. 2): (1) a fall transition period when the catchment experienced limited soil water recharge following the previous summer drought, (2) a winter low flow period when the catchment experienced minimal water input, (3) an early-melt transition period when the catchment began experiencing active snowmelt input that generated a small streamflow response, (4) a rising limb period when snowmelt in the

HESSD
10, 2549–2600, 2013

catchment generated a rapid rise in the streamflow response, (5) a peak flow period when the streamflow response reached its maximum, (6) a falling limb period when the streamflow decreased quickly and the last of the remaining snow covered areas within the catchment were melting rapidly, (7) a post-melt transition period when no snow remained in the catchment and streamflow continued decreasing at a moderate rate, and (8) a summer low flow period when streamflow responded to occasional intense rainstorm events.

Three types of response variables were defined: (1) occurrence, in which a well was assigned a value of 1 if a groundwater response was observed during the period of record and 0 if not; (2) duration, computed by determining the fractional portion of time that a water table was recorded in a well, and then reducing this interval measure to ordered classes for each time period; and (3) timing, in which the date/time (in decimal days since 1 January) of first response and maximum response were classified into ordered classes. Duration classes were defined for the eight streamflow periods individually, then for the melt period after aggregating streamflow periods 3–6, and again for the annual period after aggregating all eight streamflow periods. OLR analyses were applied to all three levels of aggregation. Observations of both transient perched groundwater and continuously persistent groundwater, which may extend deep into the subsurface, were treated as one population for the analyses regardless of the lower extent of saturation. OLR requires that the number of cases within each response class exceed the number of predictor terms in the model, which restricted the number of classes that could be defined to two or three. As much as possible, natural breaks in the distribution of the response data were used to define class thresholds, but it was necessary to adjust the thresholds slightly for each streamflow period to meet the necessary sample size for each class based on the distribution of durations in the response data. Table 3 provides a summary of the classes for each period. Applying an ordered classification to the duration data also led to a loss of information since duration does not account for variation in groundwater response intensity (e.g. maximum groundwater level, rate of rise or fall); however, it was considered more important to maximize the spatial coverage than to capture more details of the groundwater dynamics.

In total, 36 site parameters were considered as candidate predictors in the OLR models (Table 2). For each parameter, a frequency histogram was used to verify whether or not the data were normally distributed and an appropriate transformation was applied, if necessary. Although OLR does not assume any particular sampling distribution, it is known to perform better in some circumstances when the predictor variables are normally distributed (Tabachnick and Fidell, 2007), and this finding was true for the current study. All predictor variables were standardized to minimize computational issues related to multicollinearity and to enhance interpretation of the model coefficients. To reduce the number of potential predictor variables for each model, the classified response data were fit to each potential predictor variable separately and the strongest predictor variable from each parameter group (e.g. forest cover group, soil constituent group; Table 2) was selected to enter the model first. Individual variables and variable interactions were then added, removed, or replaced to achieve a final model for each streamflow period. Any effects that were not physically meaningful or possible were removed from the models. Since the groundwater wells were installed to varying depths, well depth was included as a potential predictor variable to assess whether or not the well installation depths biased the observed responses.

The Wald test statistic (Engle, 1984), the AIC (Akaike, 1987), and the Bayesian information criterion (BIC) (Schwarz, 1978) were all used for variable selection, with an emphasis on BIC, as it led to the most parsimonious models. OLR assumes that the coefficients that describe the relationship between the predictor variables and the response category are the same for each response category in a model, which is called the proportional odds assumption or the parallel regression assumption. If this assumption were not true, different sets of predictor coefficients would be required to describe the relationship with each response category. OLR assumes that the relationship between the predictor variables and the natural logarithm of the odds ratio of the response (Eq. 1) is linear. Plots of partial residuals were used to confirm that the

HESSD
10, 2549–2600, 2013

proportional odds assumption was met, to check that predictors behaved linearly, and to check for potential outliers. Lastly, a bootstrap resampling validation procedure generating Somers' D rank correlation (Somers, 1962) and R^2 index statistics was applied to assess predictive performance. For LR, R^2 is referred to as an index because the residuals in LR are always the difference between a binary value (0 or 1) and the calculated probability and, therefore, R^2 is not strictly the same in LR as in OLR. R statistical software (R Development Core Team, 2010) was used for all statistical analyses.

3 Results

3.1 Space-time patterns of water inputs to the catchment

Figure 3 shows the distribution of mean annual potential solar radiation and maps of snow cover for 2007 and 2008. Locations along the valley bottoms receive low amounts of solar energy regardless of the slope aspect due to hillslope shading. It was observed during field investigations over three years that the snowline retreat patterns were generally consistent from year to year, but with differences in timing. The general spatial pattern of spring snowline retreat and, thus, the spatial shifting of the lower extent of snowmelt input to the soil progresses as follows: (1) south-facing, low elevation clearcut areas; to (2) south-facing, middle-elevation forest and clearcut areas; to (3) south-facing, high elevation forest areas; and north-facing, low and middle elevation forest and clearcut areas; to (4) north-facing, high elevation forest areas.

3.2 Groundwater response occurrence and duration for the melt period and the annual cycle

Groundwater responses were never observed at 13 of the 50 hillslope sites in the UEC catchment. The probability of a groundwater response occurring increased with increasing upslope drainage area or with increasing melt period mean daily solar radiation, but decreased with increasing slope gradient or with increasing 75 cm depth K_s

HESSD
10, 2549–2600, 2013

(hereafter referred to as *deep soil* K_s; refer to Table 4 for the OLR models and Fig. 4 for the change in probability along each variable gradient). The odds ratio of the main effect for each predictor variable (using the difference between the 25th and 75th percentile values for each predictor variable) showed that deep soil K_s was the most important variable in determining the probability of a groundwater response occurrence followed by upslope drainage area, insolation, and slope gradient, in order of importance (refer to Fig. 5 for the strengths of the variable effects). However, accounting for variable interactions, slope gradient was found to have a highly negative effect on the probability of occurrence among low insolation sites and a weakly positive effect among high insolation sites (Figs. 4 and 5). Insolation had a strongly positive effect on the probability of occurrence among high slope gradient sites and a slightly weaker negative effect among low slope gradient sites. Inspection of the locations of the sites that did not show a groundwater response (indicated by "·" symbols in Fig. 6) shows that unresponsive sites tended to be on middle or upper hillslope locations among areas with planar surface curvature and on ridges, which is consistent with the model results. The spatial distribution of deep soil K_s was also generally consistent with the model results based on a manual comparison. The absence of unresponsive sites within the south-facing clearcut area suggests that forest cover might also be an important variable, but none of the forest cover parameters was significant in the model, possibly due to their being overwhelmed by the influence of insolation or due to statistical limitations associated with the sample size.

Over the annual period, the probability of a higher response duration increased with increasing upslope area or insolation, but decreased with increasing slope gradient, maximum tree diameter, or deep soil K_s (Fig. 4). In order of importance, the main effects were strongest for maximum tree diameter and upslope area, somewhat weaker for deep soil K_s and slope gradient, and much weaker for insolation (Fig. 5). Interaction effects showed that slope gradient had a stronger negative effect among sites with low insolation, and a weakly positive effect among sites with high insolation (Figs. 4 and 5). Insolation had a much stronger positive effect among sites with high slope gradient and

HESSD
10, 2549–2600, 2013

a strongly negative effect among sites with low slope gradient. Inspection of the spatial distribution of annual response durations (indicated by symbol size in Fig. 6) shows that sites with persistent responses tended to be located near streams or in hillslope hollows, particularly those with low slope gradients. Moreover, 36 % of the clearcut sites experienced a 0.75–1.0 response (i.e. a water table was measured within the well 75 % to 100 % of the time; largest symbol size in Fig. 6), whereas only 11 % of the forested sites experienced a > 0.75 response.

When OLR was applied to the duration of groundwater response throughout the melt period (defined as 11 April–7 June for the streamflow duration data), the variables in the model, their interactions, and their signs (i.e. positive or negative effects) were the same as for the annual duration model, but the order of importance varied (Figs. 4 and 5). In particular, slope gradient and deep soil K_s had stronger effects than both maximum tree diameter and upslope area. Moreover, the overall strengths of the main and interaction effects were stronger for slope gradient and weaker for maximum tree diameter and upslope area. Compared to the persistence of response on an annual basis, some sites that were distant from the stream network and not in well defined hillslope hollows experienced more persistent responses (Fig. 6).

3.3 Response timing analysis

For sites with groundwater responses that persisted through the winter, the date/time of the start of the first distinct rise in the water table level during the spring melt was used as the timing of first response. For other sites, the first response was defined as the date/time that a water table was first recorded in the well. The fitted OLR model showed that the timing of first response was advanced with increasing upslope drainage area or with a greater portion of the upslope area being logged, whereas the timing of first response was delayed with increasing elevation, deep soil K_s, or silt fraction (refer to Fig. 7 for the change in probability along each variable gradient and Table 5 for the strengths of the variable effects). The main effects were strongest for upslope drainage area followed by elevation, silt fraction, deep soil K_s, and upslope logging (Table 5). No

HESSD
10, 2549–2600, 2013

interaction effects were significant in the model. Inspection of the spatial distribution of first response (indicated by symbol size in Fig. 6) shows that sites with an early first response tended to be located near streams and in hillslope hollows, and in the low elevation south-facing clearcut.

When the date/time of maximum groundwater level was used as a response variable, the fitted OLR model showed that the timing of maximum response was advanced with increasing insolation and clear-sky fraction, but delayed with increasing silt fraction (Fig. 7). Clear-sky fraction was the strongest effect with much weaker effects from insolation and silt fraction, in order of importance (Table 5). No interaction effects were significant in the model. Inspection of the spatial distribution of the maximum response (indicated by symbol size in Fig. 6) shows that sites with an early maximum response tended to be located in the low elevation south-facing clearcut.

3.4 Response during individual streamflow periods

For the individual streamflow periods, OLR models for response duration included two or more of the following variables: upslope drainage area, slope gradient (mean of upslope and downslope directions or downslope direction only), deep soil K_s, maximum tree diameter, and insolation (Table 4 and Fig. 8). Three out of eight models also incorporated interactions between slope gradient and insolation. Other variables from the list of parameters that were tested (Table 2) were either not significant in the models, explained smaller amounts of variance in the data than the associated variables that were selected, or their effects were not physically meaningful. Well depth was not significant in any model. Upslope drainage area and slope gradient were important in all periods, with each holding either first or second place in terms of importance (Fig. 5), except in period 3 (early-melt transition) and period 4 (rising limb) when maximum tree diameter and deep soil K_s had the strongest effects relative to other variables, respectively. The main effects of upslope area and slope gradient were positive and negative during all periods, respectively, and were at their weakest levels during periods 3 and 4, respectively (Figs. 5 and 8).

HESSD
10, 2549–2600, 2013

Deep soil K_s had the third strongest main effect in periods 1 through 3 and 8, and the strongest effect in period 4, but was not significant in the models during periods 5 through 7 when the catchment was wet throughout and draining. Maximum tree diameter was significant in the model only during periods 1 through 4 with its importance rising to a maximum during period 3 (early-melt transition). The effects of deep soil K_s and maximum tree diameter were negative during all relevant periods. Insolation was significant in the models only during periods 3 through 5 when snowmelt was widespread throughout the catchment. The main effect of insolation was weakly positive during period 3 (early-melt transition), moderately positive during period 4 (rising limb), and moderately negative during period 5 (peak flow), showing the spatial shifting of dominant water input source areas from high insolation sites in periods 3 and 4 to low insolation sites in period 5. Moreover, the effect of insolation was strongly negative among low slope gradient sites and strongly positive among high slope gradient sites during periods 3, 4, and 5 (Figs. 5 and 8). During periods 3 through 5, the effect of slope gradient was strongly negative among sites with low insolation. Among sites with high insolation, the effect of slope gradient was weakly positive during periods 3 (early-melt transition) and 4 (rising limb), and moderately positive during period 5 (peak flow). Interestingly, sites with low slope gradient and high insolation and sites with high slope gradient (regardless of insolation) had lower overall shallow soil saturation (mean of 10–40 cm soil depth) at the start of the spring melt compared to sites with low slope gradient and low insolation (Fig. 9).

By examining the relative positions of the main effects along the respective x-axes in Fig. 8, one can observe that the relations shift to higher or lower values of the predictor variables sequentially between periods. To investigate this variation in more detail, the 0.1 and 0.5 probabilities of a persistent response are plotted for each predictor variable (except insolation since the direction of its effect, i.e. positive versus negative, changes between period 4 and period 5) and period in Fig. 10. Compared to the 0.1 probability, the 0.5 probability had a higher upslope area and lower slope gradient, deep soil K_s, and maximum tree diameter in any given period. These relative positions are consistent with the positive main effect of upslope area versus the negative main effects of slope gradient, deep soil K_s, and maximum tree diameter on the duration of groundwater response (Figs. 5 and 8). Examining a constant probability of a persistent response (e.g. 0.5), the minimum upslope area required to generate persistent groundwater responses reached a maximum in period 2 or 3 and a minimum in period 4. During period 4, probabilities of experiencing persistent groundwater responses of 0.1 and 0.5 were associated with upslope areas of approximately 90 m^2 and 1120 m^2, respectively. In contrast, the same probabilities were associated with upslope areas of approximately 1.6 ha and 140 ha during period 3, respectively. Similarly, the slope gradient associated with a particular probability of a persistent groundwater response (e.g. 0.5) reached a maximum in period 4 and a minimum in periods 2 or 3. During period 4, probabilities of 0.1 and 0.5 were associated with slope gradients of approximately 68 % and 32 %, respectively, whereas the same probabilities were associated with slope gradients of approximately 20 % and 9 % during period 3. This expansion of the groundwater response areas to locations with higher slope gradients and smaller upslope drainage areas (i.e. planar hillslopes and ridges) followed by contraction of the runoff generation areas can be observed in plots of the spatial distribution of 0.75–1.0 duration sites (i.e. responded during 75 % to 100 % of the period) between each period (Fig. 5.10 in Smith, 2011, see Supplement). The most widespread distribution occurred in period 5. It is also possible to observe that from period 3 through period 5, moderate and high elevation sites were sequentially added to the portion of sites that experienced persistent responses while a small number of low elevation sites stopped contributing.

The limiting effect of deep soil K_s on groundwater response (Fig. 10) was greatest in period 1 (i.e. only sites with very low values of K_s were likely to experience persistent groundwater responses) when the catchment was relatively dry and streamflow was low following the summer drought, and decreased (i.e. higher K_s value) in subsequent periods. Deep soil K_s was the least limiting (i.e. even sites with high values of K_s were likely to experience persistent groundwater responses) in period 4 during widespread

HESSD
10, 2549–2600, 2013

snowmelt and was insignificant in the models for periods 5 through 7. During period 1, probabilities of 0.1 and 0.5 were associated with deep soil K_s values of approximately $9 \times 10^{-9}\,\mathrm{m\,s^{-1}}$ and $5 \times 10^{-10}\,\mathrm{m\,s^{-1}}$, whereas the same probabilities were associated with deep soil K_s values of approximately $4 \times 10^{-5}\,\mathrm{m\,s^{-1}}$ and $4 \times 10^{-6}\,\mathrm{m\,s^{-1}}$ during period 4, respectively.

Maximum tree diameter was most limiting (i.e. only sites with small or no trees were likely to experience persistent groundwater responses; Fig. 10) during period 1 when the catchment was relatively dry and streamflow was low. Maximum tree diameter was least limiting (i.e. sites with small through large diameter trees were likely to experience persistent groundwater responses) in period 4 during widespread snowmelt and was insignificant in the models for periods 5 through 8. During period 1, sites with forest cover had probabilities of experiencing persistent groundwater responses that were less than 0.1, whereas probabilities of 0.1 and 0.5 were associated with maximum tree diameters of approximately 72 cm and 33 cm during period 4, respectively. The limiting effects of forest cover on melt can be observed for period 3 when sites within the low elevation south-facing clearcut area experienced persistent groundwater responses, but sites in adjacent forested areas of similar or lower elevation and similar insolation did not respond or responded minimally (Fig. 5.10 in Smith, 2011, see Supplement). For periods 4 and 5, one can observe that sites with persistent groundwater responses were distributed throughout both forested and clearcut areas.

4 Discussion

4.1 Controls on the spatial distribution of groundwater occurrence

Deep soil K_s (measured at 75 cm depth) was the most important variable for predicting whether or not a site experiences any detectable groundwater response within the range of soil depths that were monitored (i.e. groundwater well depths ranged between 0.50 m and 1.64 m). Moreover, the finding that a groundwater response is more likely to

HESSD
10, 2549–2600, 2013

occur at high slope gradient sites with high insolation compared to high slope gradient sites with low insolation, despite having negligible differences in shallow soil wetness at the start of the spring melt, suggests that water input intensity is also an important influence on the spatial distribution of the occurrence of groundwater response. These results are consistent with the percolation-excess runoff generation mechanism described by Redding and Devito (2008, 2010), who found that water input intensity was a first-order control on the occurrence and amount of lateral flux in glacial till soils due to its influence on vertical versus lateral flux partitioning. Similar results were found for the UEC catchment, as described by Smith et al. (2013). In the statistical models for this study, deep soil K_s likely accounts for variation in the depth of the percolation-limiting layer.

Upslope drainage area and slope gradient were also found to be important in determining whether or not a site experiences a detectable groundwater response. This finding suggests that some sites with large upslope areas will experience a shallow groundwater response regardless of the K_s of the surficial soils due to high rates of flow accumulation. Jencso et al. (2009) also found a positive relation between the occurrence of groundwater response and upslope drainage area for sites in a snowmelt-dominated catchment in Montana. However, notwithstanding these findings, the current study suggests that the underlying geology and the various physiographic influences on snowmelt intensity might be as important or more important than topographic convergence in determining the spatial distribution of responsive sites.

4.2 Controls on the space-time distribution of groundwater persistence

During the early phases of the spring freshet, while the catchment is relatively dry (except along riparian corridors) and snow covered, increasing energy inputs begin to generate melt in low elevation, high insolation locations of the catchment. Under these conditions, the OLR models suggest that vertical controls (i.e. localized energy and mass inputs, and vertical versus lateral flux partitioning expressed by maximum tree diameter and deep soil K_s) dominate the patterns of persistent groundwater response due to the influence of locally generated snowmelt. Once snowmelt expands throughout the catchment and most of the catchment is wet and hydrologically connected, lateral controls (i.e. lateral hydraulic gradient and flowpath convergence expressed by slope gradient and upslope contributing area) begin to dominate the persistence of groundwater response, which continues throughout the peak flow period and throughout the summer, autumn, and winter low-flow periods while the catchment drains. These findings are supported by those of Jencso et al. (2009), Jencso and McGlynn (2011), and Kuras et al. (2008) for other snowmelt-dominated montane catchments, and by those of Szeftel (2010) for the CCEW. These findings also corroborate the applicability of the generally accepted relations between soil wetness and various topographic indices (Quinn et al., 1995; Beven and Kirkby, 1979), as well as the importance of topographic position as a controlling factor in runoff generation dynamics (Dunne and Black, 1970a, b; Freeze, 1972; Hewlett and Hibbert, 1963, 1967; Sidle et al., 2000), except during the early-melt and rising limb periods of the spring freshet.

The contrast in the dominance of vertical versus lateral controls is also highlighted by the positive influence of insolation on the persistence of groundwater response at high slope gradient sites during the early-melt, rising limb, and peak flow periods compared to the negative influence at low slope gradient sites during the same periods. The same patterns exist regarding the probability of groundwater response occurrence. Low slope gradient sites on low insolation hillslopes are generally wetter at the start of the spring melt compared to low gradient sites on high insolation hillslopes (Fig. 9), likely due to lower rates of pre-melt evapotranspiration (particularly before snowpack development) and, thus, greater pre-melt accumulated soil wetness in low insolation areas than in high insolation sites. These differences appear to make low gradient, low insolation sites more responsive to water inputs than low gradient, high insolation sites, which is corroborated by field observations that north-facing areas are generally wetter throughout the snow-free season and have a higher density of streams compared to south-facing areas. In contrast, the high rates of soil drainage at high slope gradient sites likely limit the potential for evapotranspiration differences to generate large differences in antecedent soil wetness at the start of the spring melt. Thus, higher rates of snowmelt on high slope gradient, high insolation sites have a greater ability to generate a groundwater response compared to relatively lower rates of snowmelt on high slope gradient, low insolation sites. In essence, controls on antecedent wetness and flowpath convergence overwhelm controls on water input intensity and vertical versus lateral flux partitioning among low slope gradient sites, but not among high slope gradient sites.

The fact that maximum tree diameter is the most important variable in determining the persistence of groundwater response over the annual cycle is consistent with the hypothesis that forest cover removal increases groundwater levels via its negative influence on evapotranspiration and positive influence on water input.

4.3 Controls on groundwater response timing

The timing of first groundwater response is controlled by parameters influencing the upslope hydrologic conditions and lateral redistribution (e.g. the upslope drainage area, the portion of the upslope area that is logged), the local soil hydraulics (e.g. deep soil K_s, silt fraction), and the localized energy inputs and/or snowpack depth (e.g. as influenced by elevation). The strong importance of upslope drainage area shows that when the upslope area is large, even small amounts of melt can generate an initial groundwater response, likely due to the influence of lateral redistribution of soil water on antecedent wetness. The influence of upslope logging on the timing of first response is likely related to the fact that removal of forest cover results in reduced transpiration and, thus, wetter soils leading into the winter period, coupled with earlier snowmelt in the spring. A high value of deep soil K_s means that more storage capacity must be satisfied (i.e. due to greater depth to the percolation-limiting layer) before the first groundwater response can occur.

The timing of maximum groundwater response appears to be controlled primarily by parameters influencing the localized energy inputs (e.g. clear-sky fraction, insolation) with less control by parameters influencing the local soil hydraulics (e.g. only silt fraction is important) and negligible control related to lateral redistribution. Neither upslope drainage area nor slope gradient are important controls on the timing of maximum groundwater response, suggesting that the timing of maximum response is determined more by vertical process controls than by lateral process controls, which is consistent with the maximum response being controlled more by surface processes. The importance of clear-sky fraction and insolation in controlling the timing of maximum response illustrates the importance of localized energy and mass flux dynamics on the differential timing, intensity, and quantity of snowmelt and their subsequent influences on the timing of response. Overall, the controls on both timings (i.e. first and maximum groundwater responses) have some consistency with the controls on snow accumulation and melt processes, particularly for the timing of maximum groundwater response.

4.4 Implications for runoff source area dynamics and catchment modelling

Sites with high values of deep soil K_s that do not generate a shallow groundwater response should experience deep percolation and likely generate runoff via slow response pathways, resulting in continual drainage throughout the recession and low flow periods. These findings are supported by two points: (1) precipitation exceeds actual evapotranspiration in the UEC catchment and, therefore, all sites must experience runoff (ignoring the influences of wind redistribution, which is negligible under a forest canopy, on the water balance); and (2) rapid response pathways within the deep subsoil, such as deep soil cracks in clay or bedrock (Montgomery et al., 1997, 2002; Tromp-van Meerveld et al., 2007), are likely limited in abundance since the soils are deep (in excess of 8 m in some areas) with only small amounts of clay and minimal bedrock. Thus, the spatial distribution of surficial soil K_s is an important control on the distribution of sites that generate rapid runoff versus sites that generate slow runoff. Consistent with our findings, Kuras et al. (2008) found that runoff source area dynamics during low flow periods were not explained well by surface topography and suggested that deep, disconnected flows dominate runoff generation during these periods. Jencso and McGlynn (2011) found that increasing proportions of permeable geology

HESSD
10, 2549–2600, 2013

underlying relatively wet landscapes were correlated with decreased streamflow yield per unit length of hillslope hydrologic connectivity during wet periods and enhanced yield during dry periods. Moreover, sites with large upslope drainage areas and high values of soil K_s that also experience a shallow groundwater response would be capable of transmitting water to the stream network at a high rate and, thus, would be critical in the connectivity of runoff source areas to streams.

The amount of incident solar radiation differentiates runoff source areas during the early-melt period and, to a lesser extent, during the rising limb and peak flow periods. However, its influence weakens as active snowmelt zones shift into more shaded (via topography and/or forest cover) locations. Peak streamflow occurs when snowmelt and runoff are being generated throughout most areas of the catchment, including locations with low insolation, with mature forest cover, with high slope gradients, with convex topography (i.e. ridges), and with high elevations (Fig. 10 and Fig. 5.10 in Smith, 2011, see Supplement). This expansion and contraction of the runoff source areas is analogous to the patterns described by conceptual rainfall runoff models (Dunne and Black, 1970a, b; Freeze, 1972; Hewlett and Hibbert, 1963, 1967; Sidle et al., 2000), and is consistent with the findings of Jencso et al. (2009), Kendall et al. (1999), and Kuras et al. (2008).

Topography-based indices (Beven and Kirkby, 1979; Quinn et al., 1995) and the various rainfall runoff conceptual models (Dunne and Black, 1970a,b; Freeze, 1972; Hewlett and Hibbert, 1963, 1967; Sidle et al., 2000) should be reliable predictors of runoff source area dynamics in snowmelt-dominated montane catchments during peak flow, recession flow, and low flow periods since upslope area and slope gradient were dominant in the statistical models during these periods (Jencso and McGlynn, 2011; Jencso et al., 2009; Kuras et al., 2008; Szeftel, 2010). However, they would likely be poor predictors of runoff source area dynamics during early phases of the spring freshet without adequately addressing the space-time variability of water input intensity (i.e. controls on snowpack conditions and surface energy fluxes). Kuras et al. (2008) found that differential snowmelt timing between clearcuts and forested

HESSD
10, 2549–2600, 2013

areas was responsible for generating different streamflow peaks. Moreover, for glacial till catchments with spatially variable soil K_s profiles or for catchments with varying soil depths, catchment models must address the spatial distribution of controls on vertical versus lateral flux partitioning in the soil coupled with the distribution of controls on the rate of percolation to adequately explain runoff source area dynamics during all periods, including differentiation of rapid runoff response areas from areas that contribute primarily to sustaining low flows (Redding and Devito, 2008, 2010).

5 Conclusions

The spatial controls on the occurrence, timing, and persistence of shallow groundwater response in glacial till montane catchments that are snowmelt-dominated are complex and vary not only between seasons, but also intra-seasonally. The K_s of the soil at 75 cm depth was found to be a first-order control on the distribution of sites that generate shallow groundwater response versus sites that experience only deep percolation. Moreover, the study findings suggest that sites with highly permeable surface soils, large upslope contributing areas, and low slope gradients would be important links in the connectivity of runoff source areas to streams. Upslope contributing area and slope gradient are first-order controls on the persistence of groundwater response during peak flow, recession flow, and low flow periods. Runoff source areas expand and contract throughout these periods according to an interplay between catchment wetness and the spatial patterns of topographic convergence; however, controls on the differential timing, intensity, and quantity of snowmelt and controls on vertical versus lateral flux partitioning in the soil overwhelm the influence of topographic convergence on runoff source area dynamics during early spring freshet periods. These findings suggest that various topographic indices and topography-based rainfall runoff models are not directly applicable to modelling snowmelt runoff source area dynamics during all streamflow periods. Topography-based indices would likely be poor predictors of runoff source area dynamics during early phases of the spring freshet without adequately

HESSD
10, 2549–2600, 2013

addressing controls on the space-time variability of water input intensity and the spatial distribution of controls on vertical versus lateral flux partitioning in the soil and rate of percolation.

Supplementary material related to this article is available online at: http://www.hydrol-earth-syst-sci-discuss.net/10/2549/2013/ hessd-10-2549-2013-supplement.pdf.

Acknowledgements. We would like to thank the following for assistance with the field study and logistical support: Georg Jost, Dave Gluns, Pascal Szeftel, Michelle Sawka, Gerard Lohmann, Ryan Thoren, Nils Illchman, Natalie Stafl, Maria Staudinger, Fabian Nippgen, Nicolas Teichrob, Selina Agbayani, Kyle Terry, Roger Hodson, Stephanie Ewen, Vojtech Prilesky, Andres Varhola, Amy O'Neil, Jason Leach, Kim Green, Younes Alila, Diana Allen, Harry Verwoerd, Jerry Maedel, Vincent Kujala, Julie Ranada, and Nicholas Coops. Eric Leinburger provided cartographic assistance. Important funding and/or logistical support was provided by Tembec Inc., B.C. Ministry of Forests and Range, Forest Investment Account – Forest Sciences Program (grant nos. Y062294, Y081214), Kalesnikoff Lumber Co. Ltd., Alberta Pacific Forest Industries Inc., Natural Sciences and Engineering Research Council of Canada, Mathematics of Information Technology and Complex Systems Network of Centres of Excellence, Sustainable Forest Management Network, and the University of Zürich.

References

Akaike, H.: Factor-analysis and AIC, Psychometrika, 52, 317–332, 1987.

Ali, G., L'Heureux, C., Roy, A. G., Turmel, M. C., and Courchesne, F.: Linking spatial patterns of perched groundwater storage and stormflow generation processes in a headwater forested catchment, Hydrol. Process., 25, 3843–3857, doi:10.1002/hyp.8238, 2011.

Anderson, M. G. and Burt, T. P.: The role of topography in controlling throughflow generation, Earth Surf. Proc. Land., 3, 331–344, 1978.

Anderton, S. P., White, S. M., and Alvera, B.: Micro-scale spatial variability and the timing of snow melt runoff in a high mountain catchment, J. Hydrol., 268, 158–176, 2002.
AquaPro Sensors: Reno, NV, AquaPro Sensors is the issuing organization, available at: www.aquapro-sensors.com, 2012.
Balk, B. and Elder, K.: Combining binary decision tree and geostatistical methods to estimate snow distribution in a mountain watershed, Water Resour. Res., 36, 13–26, 2000.
BC Geological Survey: Victoria, BC, Ministry of Energy, Mines, and Natural Gas, 2012.
Berris, S. N. and Harr, R. D.: Comparative snow accumulation and melt during rainfall in forested and clear-cut plots in the Western Cascades of Oregon, Water Resour. Res., 23, 135–142, 1987.
Beschta, R. L., Pyles, M. R., Skaugset, A. E., and Surfleet, C. G.: Peakflow responses to forest practices in the western cascades of Oregon, USA, J. Hydrol., 233, 102–120, 2000.
Beven, K. J. and Kirkby, M. J.: A physically-based variable contributing area model of basin hydrology, Hydrol. Sci. Bull., 24, 43–69, 1979.
Boyer, E. W., Hornberger, G. M., Bencala, K. E., and McKnight, D. M.: Variation of dissolved organic carbon during snowmelt in soil and stream waters of two headwater catchments, Summit County, Colorado, in: Biogeochemistry of Seasonally Snow-Covered Catchments, edited by: Tonnessen, K. A., Williams, M. W., and Tranter, M., IAHS Publications, 228, 303–312, From international union of geodesy and geophysics general assembly Boulder, Colorado, USA, 2–14 July, 1995.
Boyer, E. W., Hornberger, G. M., Bencala, K. E., and McKnight, D. M.: Response characteristics of DOC flushing in an alpine catchment, Hydrol. Process., 11, 1635–1647, 1997.
Boyer, E. W., Hornberger, G. M., Bencala, K. E., and McKnight, D. M.: Effects of asynchronous snowmelt on flushing of dissolved organic carbon: a mixing model approach, Hydrol. Process., 14, 3291–3308, 2000.
Buttle, J. M.: Isotope hydrograph separations and rapid delivery of pre-event water from drainage basins, Prog. Phys. Geog., 18, 16–41, 1994.
Buttle, J. M., Dillon, P. J., and Eerkes, G. R.: Hydrologic coupling of slopes, riparian zones and streams: an example from the Canadian Shield, J. Hydrol., 287, 161–177, doi:10.1016/j.jhydrol.2003.09.022, 2004.
Daly, S. F., Davis, R., Ochs, E., and Pangburn, T.: An approach to spatially distributed snow modelling of the Sacramento and San Joaquin basins, California, Hydrol. Process., 14, 3257–3271, 2000.

Dataflow Systems Pty Limited: Christchurch, New Zealand, 2012.
Decagon Devices Inc.: Pullman, WA, 2012.
Deng, Y., Flerchinger, G. N., and Cooley, K. R.: Impacts of spatially and temporally varying snowmelt on subsurface flow in a mountainous watershed 2: subsurface processes, Hydrol. Sci. J., 39, 521–533, 1994.
Dunne, T. and Black, R. D.: Partial area contributions to storm runoff in a small new-england watershed, Water Resour. Res., 6, 1296–1311, 1970a.
Dunne, T. and Black, R. D.: An experimental investigation of runoff production in permeable soils, Water Resour. Res., 6, 478–490, 1970b.
Dunne, T. and Black, R. D.: Runoff processes during snowmelt, Water Resour Res, 7, 1160–1172, 1971.
Engle, R. F.: Wald, likelihood ratio, and Lagrange multiplier tests in econometrics, in: Handbook of Econometrics, edited by: Griliches, Z. and Intriligator, 1st Edn., Vol. 2, Ch. 13, M. D., Elsevier, New York, 775–826, 1984.
ESRI: Redlands, CA, 2012.
Flerchinger, G. N. and Cooley, K. R.: A ten-year water balance of a mountainous semi-arid watershed, J. Hydrol., 237, 86–99, 2000.
Freer, J., McDonnell, J. J., Beven, K. J., Peters, N. E., Burns, D. A., Hooper, R. P., Aulenbach, B., and Kendall, C.: The role of bedrock topography on subsurface storm flow, Water Resour. Res., 38, 1269, doi:10.1029/2001wr000872, 2002.
Freeze, R. A.: Role of subsurface flow in generating surface runoff 2: upstream source areas, Water Resour. Res., 8, 1272–1283, 1972.
Goodrich, D. C., Faures, J. M., Woolhiser, D. A., Lane, L. J., and Sorooshian, S.: Measurement and analysis of small-scale convective storm rainfall variability, J. Hydrol., 173, 283–308, 1995.
Guan, H., Wilson, J. L., and Makhnin, O.: Geostatistical mapping of mountain precipitation incorporating autosearched effects of terrain and climatic characteristics, J. Hydrometeorol., 6, 1018–1031, 2005.
Hewlett, J. D. and Hibbert, A. R.: Moisture and energy conditions within a sloping soil mass during drainage, J. Geophys. Res., 68, 1081–1087, 1963.
Hewlett, J. D. and Hibbert, A. R.: Factors affecting the response of small watersheds to precipitation in humid areas, International Symposium on Forest Hydrology, Pergamon, Oxford, 275–290, Pennsylvania State University, 1967.

HESSD
10, 2549–2600, 2013

Hock, R.: A distributed temperature-index ice and snowmelt model including potential direct solar radiation, J. Glaciol., 45, 101–111, 1999.
Hrachowitz, M. and Weiler, M.: Uncertainty of precipitation estimates caused by sparse gauging networks in a small, mountainous watershed, J. Hydrol. Eng., 16, 460–471, 2011.
Jencso, K. G. and McGlynn, B. L.: Hierarchical controls on runoff generation: topographically driven hydrologic connectivity, geology, and vegetation, Water Resour. Res., 47, W11527, doi:10.1029/2011WR010666, 2011.
Jencso, K. G., McGlynn, B. L., Gooseff, M. N., Wondzell, S. M., Bencala, K. E., and Marshall, L. A.: Hydrologic connectivity between landscapes and streams: transferring reach- and plot-scale understanding to the catchment scale, Water Resour. Res., 45, W04428, doi:10.1029/2008wr007225, 2009.
Jost, G., Weiler, M., Gluns, D. R., and Alila, Y.: The influence of forest and topography on snow accumulation and melt at the watershed-scale, J. Hydrol., 347, 101–115, 2007.
Jost, G., Moore, R. D., Weiler, M., Gluns, D. R., and Alila, Y.: Use of distributed snow measurements to test and improve a snowmelt model for predicting the effect of forest clear-cutting, J. Hydrol., 376, 94–106, doi:10.1016/j.jhydrol.2009.07.017, 2009.
Kendall, K. A., Shanley, J. B., and McDonnell, J. J.: A hydrometric and geochemical approach to test the transmissivity feedback hypothesis during snowmelt, J. Hydrol., 219, 188–205, 1999.
Kim, J. K., Sidle, R. C., Moore, R. D., and Hudson, R.: Throughflow variability during snowmelt in a forested mountain catchment, coastal British Columbia, Canada, Hydrol. Process., 18, 1219–1236, 2004.
Kuras, P. K., Weiler, M., and Alila, Y.: The spatiotemporal variability of runoff generation and groundwater dynamics in a snow-dominated catchment, J. Hydrol., 352, 50–66, doi:10.1016/j.jhydrol.2007.12.021, 2008.
Laudon, H., Seibert, J., Kohler, S., and Bishop, K.: Hydrological flow paths during snowmelt: congruence between hydrometric measurements and oxygen 18 in meltwater, soil water, and runoff, Water Resour. Res., 40, W03102, doi:10.1029/2003wr002455, 2004.
Linderson, M. L.: Spatial distribution of meso-scale precipitation in Scania, southern Sweden, Geogr. Ann. A, 85, 183–196, 2003.
Marks, D., Winstral, A., and Seyfried, M.: Simulation of terrain and forest shelter effects on patterns of snow deposition, snowmelt and runoff over a semi-arid mountain catchment, Hydrol. Process., 16, 3605–3626, doi:10.1002/hyp.1237, 2002.

HESSD
10, 2549–2600, 2013

Runoff dynamics in a snowmelt catchment

R. S. Smith et al.

McCullagh, P.: Regression models for ordinal data, J. Roy. Stat. Soc. B Met., 42, 109–142, 1980.

McDaniel, P. A., Regan, M. P., Brooks, E., Boll, J., Bamdt, S., Falen, A., Young, S. K., and Hammel, J. E.: Linking fragipans, perched water tables, and catchment-scale hydrological processes, Catena, 73, 166–173, doi:10.1016/j.catena.2007.05.011, 2008.

McGlynn, B. L., McDonnell, J. J., Shanley, J. B., and Kendall, C.: Riparian zone flowpath dynamics during snowmelt in a small headwater catchment, J. Hydrol., 222, 75–92, 1999.

McNamara, J. P., Chandler, D., Seyfried, M., and Achet, S.: Soil moisture states, lateral flow, and streamflow generation in a semi-arid, snowmelt-driven catchment, Hydrol. Process., 19, 4023–4038, doi:10.1002/hyp.5869, 2005.

Mitchell, J. K.: Fundamentals of Soil Behavior, 2nd Edn., John Wiley & Sons, Inc., New York, 437 pp., 1993.

Monteith, S. S., Buttle, J. M., Hazlett, P. W., Beall, F. D., Semkin, R. G., and Jeffries, D. S.: Paired-basin comparison of hydrological response in harvested and undisturbed hardwood forests during snowmelt in central Ontario: I. streamflow, groundwater and flowpath behaviour, Hydrol. Process., 20, 1095–1116, doi:10.1002/hyp.5956, 2006a.

Monteith, S. S., Buttle, J. M., Hazlett, P. W., Beall, F. D., Semkin, R. G., and Jeffries, D. S.: Paired-basin comparison of hydrologic response in harvested and undisturbed hardwood forests during snowmelt in central Ontario: I I. Streamflow sources and groundwater residence times, Hydrol Process., 20, 1117–1136, doi:10.1002/hyp.6073, 2006b.

Montgomery, D. R., Dietrich, W. E., Torres, R., Anderson, S. P., Heffner, J. T., and Loague, K.: Hydrologic response of a steep, unchanneled valley to natural and applied rainfall, Water Resour. Res., 33, 91–109, 1997.

Montgomery, D. R., Dietrich, W. E., and Heffner, J. T.: Piezometric response in shallow bedrock at CB1: implications for runoff generation and landsliding, Water Resour. Res., 38, 1274, doi:10.1029/2002wr001429, 2002.

Penna, D., Tromp-van Meerveld, H. J., Gobbi, A., Borga, M., and Dalla Fontana, G.: The influence of soil moisture on threshold runoff generation processes in an alpine headwater catchment, Hydrol. Earth Syst. Sci., 15, 689–702, doi:10.5194/hess-15-689-2011, 2011.

Quinn, P. F., Beven, K. J., and Lamb, R.: The ln(A/tanB) index: how to calculate it and how to use it within the topmodel framework, Hydrol. Process., 9, 161–182, 1995.

R Development Core Team: R: a language and environment for statistical computing, in: R Foundation for Statistical Computing, Vienna, Austria, 2010.

Redding, T. E. and Devito, K. J.: Lateral flow thresholds for aspen forested hillslopes on the Western Boreal Plain, Alberta, Canada, Hydrol. Process., 22, 4287–4300, doi:10.1002/hyp.7038, 2008.

Redding, T. E. and Devito, K. J.: Mechanisms and pathways of lateral flow on aspen-forested, Luvisolic soils, Western Boreal Plains, Alberta, Canada, Hydrol. Process., 24, 2995–3010, doi:10.1002/hyp.7710, 2010.

Rivix LLC: RiverTools topographic and river network analysis, Broomfield, CO, 2012.

SAGA User Group Association: System for Automated Geoscientific Analyses, Hamburg, Germany, 2012.

Schwarz, G.: Estimating the dimension of a model, Ann. Stat., 6, 461–464, 1978.

Seibert, J., Bishop, K., Rodhe, A., and McDonnell, J. J.: Groundwater dynamics along a hillslope: a test of the steady state hypothesis, Water Resour. Res., 39, 1014, doi:10.1029/2002wr001404, 2003.

Shoji, T. and Kitaura, H.: Statistical and geostatistical analysis of rainfall in central Japan, Comput. Geosci., 32, 1007–1024, doi:10.1016/j.cageo.2004.12.012, 2006.

Sidle, R. C., Tsuboyama, Y., Noguchi, S., Hosoda, I., Fujieda, M., and Shimizu, T.: Stormflow generation in steep forested headwaters: a linked hydrogeomorphic paradigm, Hydrol. Process., 14, 369–385, 2000.

Sklash, M. G. and Farvolden, R. N.: The role of groundwater in storm runoff, J. Hydrol., 43, 45–65, 1979.

Smith, R. S.: Space-time dynamics of runoff generation in a snowmelt-dominated montane catchment, PhD thesis, Department of Geography, University of British Columbia, Vancouver, BC, 170 pp., https://circle.ubc.ca/handle/2429/38132, last access: October, 2011.

Smith, R. S., Weiler, M., Moore, R. D., and Flerchinger, G. N.: Influences of water input dynamics and hydraulic conductivity on percolation-excess runoff generation, Water Resour. Res., in review, 2013.

Soil Moisture Equipment Corp: 2800 KI Guelph Permeameter operating instructions, Santa Barbara, CA, 28, 1991.

Somers, R. H.: A new asymmetric measure of association for ordinal variables, Am. Sociol. Rev., 27, 799–811, 1962.

Stadler, D., Wunderli, H., Auckenthaler, A., and Fluhler, H.: Measurement of frost-induced snowmelt runoff in a forest soil, Hydrol. Process., 10, 1293–1304, 1996.

Stein, J., Proulx, S., and Levesque, D.: Forest floor frost dynamics during spring snowmelt in a boreal forested basin, Water Resour. Res., 30, 995–1007, 1994.

Stewart, I. T.: Changes in snowpack and snowmelt runoff for key mountain regions, Hydrol. Process., 23, 78–94, doi:10.1002/hyp.7128, 2009.

Stewart, I. T., Cayan, D. R., and Dettinger, M. D.: Changes toward earlier streamflow timing across western North America, J. Climate, 18, 1136–1155, 2005.

Szeftel, P.: Stream-catchment connectivity and streamflow dynamics in montane landscapes, PhD thesis, Department of Geography, Univeristy of British Columbia, Vancouver, BC, 153 pp., 2010.

Szeftel, P., Moore, R. D., and Weiler, M.: Influence of distributed flow losses and gains on the estimation of transient storage parameters from stream tracer experiments, J. Hydrol., 396, 277–291, 2011.

Tabachnick, B. G. and Fidell, L. S.: Using Multivariate Statistics, 5th Edn., Pearson Education, Inc., Boston, USA, 980 pp., 2007.

Taupin, J. D.: Characterization of rainfall spatial variability at a scale smaller than 1 km in a semi-arid area (region of Niamey, Niger), Comptes rendus de l'Académie des sciences, Série 2, Sciences de la terre et des planètes, 325, 251–256, 1997.

Thompson, J. C. and Moore, R. D.: Relations between topography and water table depth in a shallow forest soil, Hydrol. Process., 10, 1513–1525, 1996.

Toews, D. A. A. and Gluns, D. R.: Snow accumulation and ablation on adjacent forested and clearcut sites in Southeastern British Columbia, in: Proceedings, 54th Western Snow Conference, Pheonix, Arizona, 15–17 April 1986, 101–111, 1986.

Tromp-van Meerveld, I. and McDonnell, J. J.: Threshold relations in subsurface stormflow: 1. A 147-storm analysis of the Panola hillslope, Water Resour. Res., 42, W02410, doi:10.1029/2004wr003778, 2006a.

Tromp-van Meerveld, I. and McDonnell, J. J.: Threshold relations in subsurface stormflow: 2. The fill and spill hypothesis, Water Resour. Res., 42, W02411, doi:10.1029/2004wr003800, 2006b.

Tromp-van Meerveld, I., Peters, N. E., and McDonnell, J. J.: Effect of bedrock permeability on subsurface stormflow and the water balance of a trenched hillslope at the Panola Mountain Research Watershed, Georgia, USA, Hydrol. Process., 21, 750–769, doi:10.1002/hyp.6265, 2007.

Winkler, R. D., Spittlehouse, D. L., and Golding, D. L.: Measured differences in snow accumulation and melt among clearcut, juvenile, and mature forests in southern British Columbia, Hydrol. Process., 19, 51–62, 2005.

HESSD
10, 2549–2600, 2013

Table 1. Data collection infrastructure at the streamflow, hillslope, and lysimeter sites.

Data Type	Site Type	Data Frequency	Equipment	Additional Details
Stream discharge	Streamflow sites	30 min	90° v-notch weir, stand pipe, and Odyssey capacitance water level recorder	Main outlet uses a naturally constricted cross-section instead of a v-notch weir
Water table elevation	Hillslope and lysimeter sites	30 min	Groundwater well and Odyssey capacitance water level recorder	Screened to $\sim$8 cm below soil surface
Soil wetness (manual)	Hillslope and lysimeter sites	Weekly to bi-monthly	AquaPro capacitance soil moisture sensor	10 cm depth intervals
Water input rate	Lysimeter sites only	Hourly	Snowmelt lysimeter with tipping bucket gauge	See study design section of main text
Air temperature	Lysimeter sites only	Hourly	ECH_20 ECT temperature sensor	2 m above soil surface

HESSD
10, 2549–2600, 2013

Table 2. Table of physiographic parameters and corresponding transformations applied for the logistic regression analyses. Parameter symbols are used in Table 4.

Parameter group	Parameter name	Transformation	Symbol
Well depth	Well depth		
Forest cover	Tree height – mean	$(x+1)^{1/3}$	
	Tree height – median	$(x+1)^{1/3}$	
	Tree height – 75th percentile		
	Tree height – 90th percentile		
	Tree height – maximum		
	Tree diameter – mean		
	Tree diameter – median	$(x+1)^{1/2}$	
	Tree diameter – 75th percentile		
	Tree diameter – 90th percentile		
	Tree diameter – maximum	$(x+1)^{1/2}$	D_{max}
	Tree basal area	$(x+1)^{1/2}$	
	Logged portion of upslope area		L
	Clear-sky fraction	$\ln(x)$	CS
Slope gradient	Slope gradient – upslope	$x^{1/2}$	
	Slope gradient – downslope	$x^{1/2}$	S_{down}
	Slope gradient – mean	$\ln(x)$	S_{mean}
Flowpath convergence	Surface curvature – plan		
	Surface curvature – profile		
	Surface curvature – mean	$(x+5.5)^{1/2}$	
	Upslope drainage area	$\ln(x)$	A
Topographic position	Elevation		E
	Elevation above channel	$x^{1/3}$	
	Elevation below ridge	$x^{1/3}$	
Insolation	Insolation – accumulation season		
	Insolation – melt season	x^2	R_{melt}
	Insolation – snow-free season		
Soil constituent	Porosity		
	Sand fraction		
	Silt fraction		SI
	Clay fraction		
	Organic fraction	$\ln(x)$	
	Coarse fragment fraction		
Soil conductivity	K_s at 25 cm soil depth	$\ln(x)$	
	K_s at 50 cm soil depth	$\ln(x)$	
	K_s at 75 cm soil depth	$\ln(x)$	K_{75}

HESSD
10, 2549–2600, 2013

Table 3. Breakdown of groundwater response classes for the occurrence of response, the duration of response (annual period, melt period, and periods 1 through 8), and the timing of response (first response or maximum response). Units for duration data are portion of period. Units for timing data are decimal day of year.

Period/timing	Range of responses		
	Class 0	Class 1	Class 2
Occurrence	0	NA	1
Annual	0	0.01–0.32	0.36–1
Melt season	0	0.01–0.46	0.56–1
1	0	0.01–0.40	1
2	0	NA	0.35–1
3	0	0.01–0.45	0.59–1
4	0	0.03–0.37	0.58–1
5	0	0.05–0.83	1
6	0	NA	0.66–1
7	0	0.34–0.80	0.93–1
8	0	0.01–0.53	0.73–1
First	102.6–105.6	119.6–127.0	137.7–140.9
Maximum	105.7–128.6	136.7–139.8	141.5–151.6

HESSD
10, 2549–2600, 2013

Table 4. Ordinal logistic regression models for the occurrence of response, the duration of response (annual period, melt period, and periods 1 through 8), and the timing of response (first response or maximum response). See Table 2 for definition of the predictor variable symbols.

Period/timing	Model	R^2	*p*-value
Occurrence	$\ln(O) = 1.92 - 1.08 \cdot S_{\mathrm{mean}} + 1.43 \cdot A - 2.83 \cdot K_{75} + 0.88 \cdot R_{\mathrm{melt}} + 1.43 \cdot S_{\mathrm{mean}} \cdot R_{\mathrm{melt}}$	0.71	< 0.001
Annual	$\ln(O) = -7.75 - 2.27 \cdot S_{\mathrm{mean}} + 2.80 \cdot A - 2.85 \cdot K_{75} + 0.48 \cdot R_{\mathrm{melt}} - 2.79 \cdot D_{\mathrm{max}} + 2.43 \cdot S_{\mathrm{mean}} \cdot R_{\mathrm{melt}}$	0.88	< 0.001
Melt	$\ln(O) = -2.44 - 3.16 \cdot S_{\mathrm{mean}} + 1.90 \cdot A - 2.66 \cdot K_{75} - 0.62 \cdot R_{\mathrm{melt}} - 1.93 \cdot D_{\mathrm{max}} + 3.26 \cdot S_{\mathrm{mean}} \cdot R_{\mathrm{melt}}$	0.86	< 0.001
1	$\ln(O) = -7.39 - 5.26 \cdot S_{\mathrm{down}} + 4.36 \cdot A - 2.18 \cdot K_{75} - 1.35 \cdot D_{\mathrm{max}}$	0.88	< 0.001
2	$\ln(O) = -5.49 - 3.51 \cdot S_{\mathrm{down}} + 2.68 \cdot A - 2.26 \cdot K_{75} - 1.67 \cdot D_{\mathrm{max}}$	0.86	< 0.001
3	$\ln(O) = -2.96 - 1.91 \cdot S_{\mathrm{down}} + 1.14 \cdot A - 2.39 \cdot K_{75} + 0.31 \cdot R_{\mathrm{melt}} - 3.22 \cdot D_{\mathrm{max}} + 1.64 \cdot S_{\mathrm{down}} \cdot R_{\mathrm{melt}}$	0.85	< 0.001
4	$\ln(O) = 0.09 - 1.24 \cdot S_{\mathrm{mean}} + 2.02 \cdot A - 2.73 \cdot K_{75} + 1.15 \cdot R_{\mathrm{melt}} - 1.21 \cdot D_{\mathrm{max}} + 1.78 \cdot S_{\mathrm{mean}} \cdot R_{\mathrm{melt}}$	0.76	< 0.001
5	$\ln(O) = -0.25 - 2.29 \cdot S_{\mathrm{mean}} + 1.88 \cdot A - 1.23 \cdot R_{\mathrm{melt}} + 2.76 \cdot S_{\mathrm{mean}} \cdot R_{\mathrm{melt}}$	0.69	< 0.001
6	$\ln(O) = -1.80 - 3.70 \cdot S_{\mathrm{down}} + 3.94 \cdot A$	0.84	< 0.001
7	$\ln(O) = -3.53 - 2.80 \cdot S_{\mathrm{down}} + 2.68 \cdot A$	0.75	< 0.001
8	$\ln(O) = -4.48 - 2.89 \cdot S_{\mathrm{down}} + 3.27 \cdot A - 2.36 \cdot K_{75}$	0.82	< 0.001
First	$\ln(O) = -3.44 - 3.63 \cdot A + 2.51 \cdot K_{75} + 2.54 \cdot E - 2.41 \cdot L + 2.95 \cdot \mathrm{SI}$	0.83	< 0.001
Maximum	$\ln(O) = -1.09 - 1.04 \cdot R_{\mathrm{melt}} - 2.73 \cdot \mathrm{CS} + 1.09 \cdot \mathrm{SI}$	0.70	< 0.001

HESSD
10, 2549–2600, 2013

Runoff dynamics in a snowmelt catchment

R. S. Smith et al.

Table 5. Ranked main effect sizes for the logistic regression models predicting response timing. Effect sizes were calculated by taking the exponential of the product of the coefficient and the range in the data between the 25th and 75th percentile values for each respective predictor variable.

Effect size	Streamflow response timing	
	Start	Maximum
> 100	– Area upslope	– Clear-sky fraction
50–100		
10–50	+ Elevation + Silt fraction +75 cm K_s – Upslope logging	
5–10		– Solar
1–5		+ Silt fraction

HESSD
10, 2549–2600, 2013

Runoff dynamics in a snowmelt catchment

R. S. Smith et al.

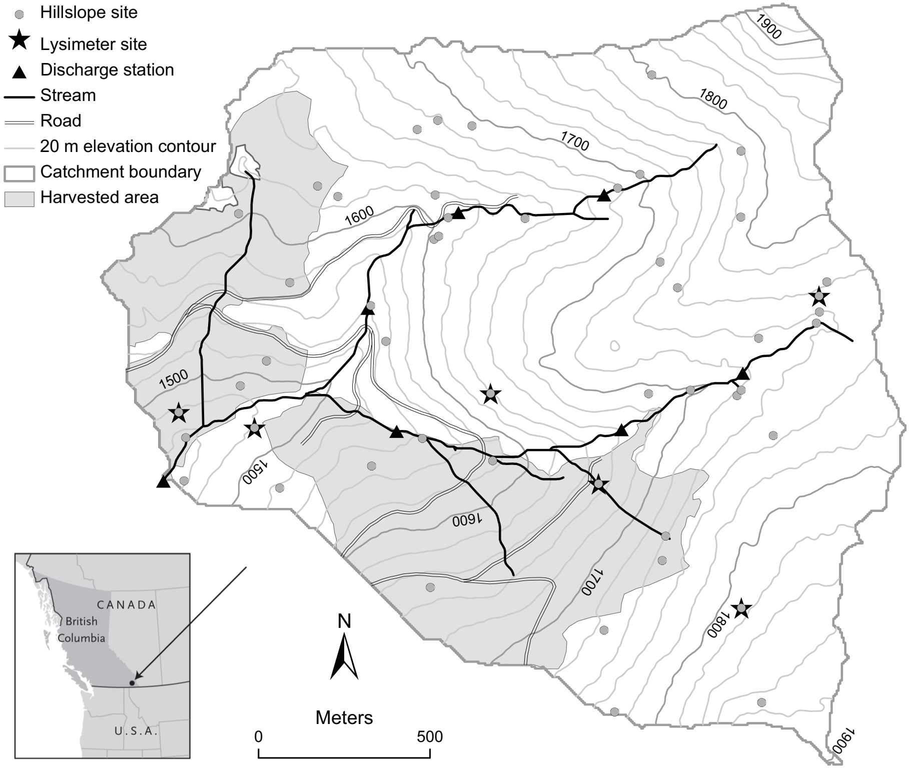

Fig. 1. Location and study sites of the Upper Elk Creek catchment.

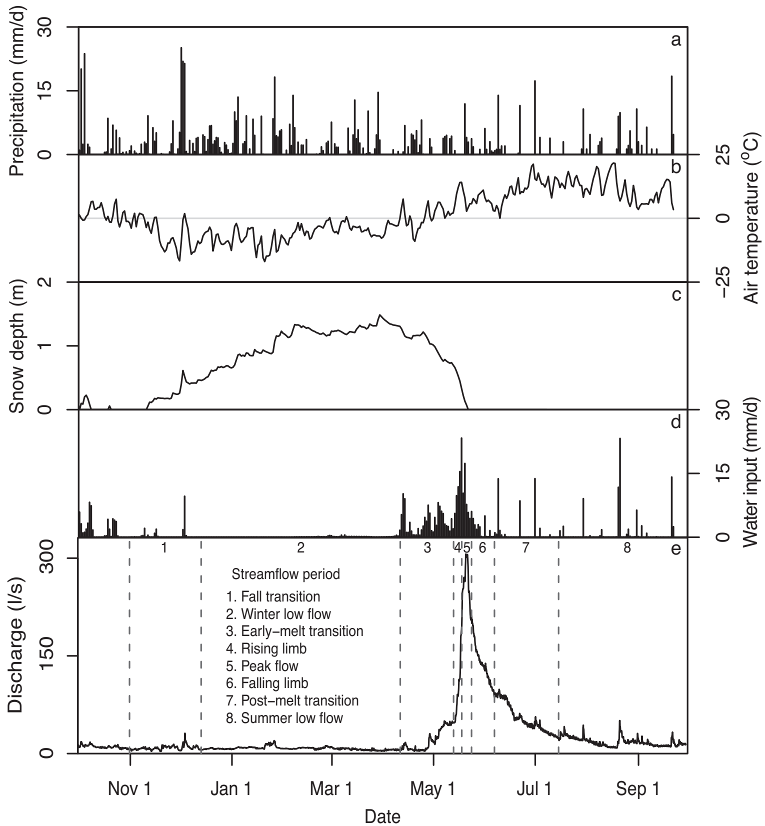

Fig. 2. Precipitation and snow depth at the UC climate station throughout the period of record, air temperature and water input as means among all six lysimeter sites in the UEC catchment, and streamflow and corresponding periods throughout the period of record at the UEC catchment outlet. The annual streamflow period is the sum of periods 1 through 8. The spring melt streamflow period is the sum of periods 3 through 6.

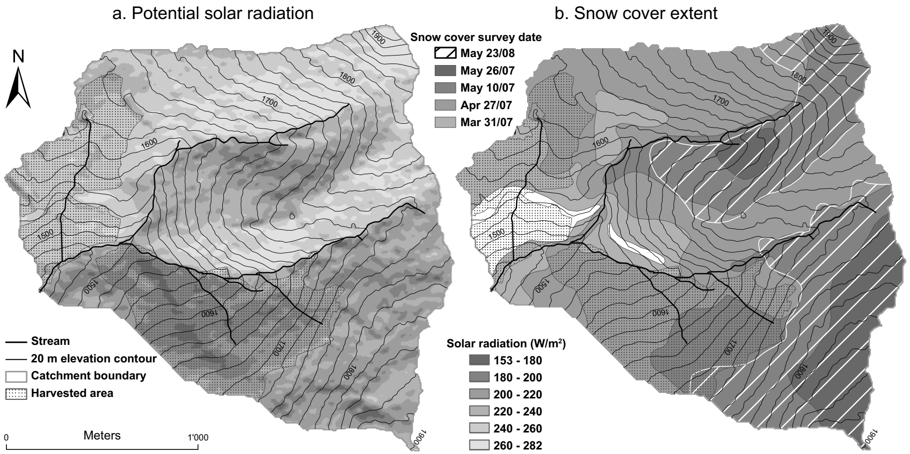

Fig. 3. Mean annual potential solar radiation **(a)** and snow cover extent during the spring melt periods of 2007 and 2008 **(b)**.

HESSD
10, 2549–2600, 2013

Runoff dynamics in a snowmelt catchment

R. S. Smith et al.

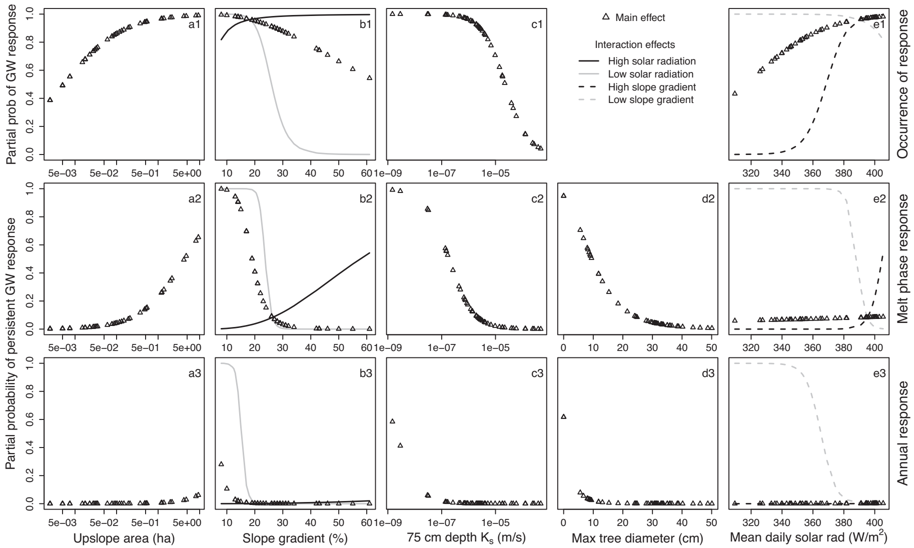

Fig. 4. Partial probability of groundwater response for each variable in the respective logistic regression models. Response periods are indicated on the far right side of each row. Response variable for row 1 is the occurrence of a groundwater response. Response variables for rows 2 and 3 are the persistence of groundwater response. For calculating the partial probabilities, all predictor variables were held at their respective mean (geometric mean for K_s) values except any relevant interaction predictor variables, which were held at their respective minimum or maximum values.

HESSD
10, 2549–2600, 2013

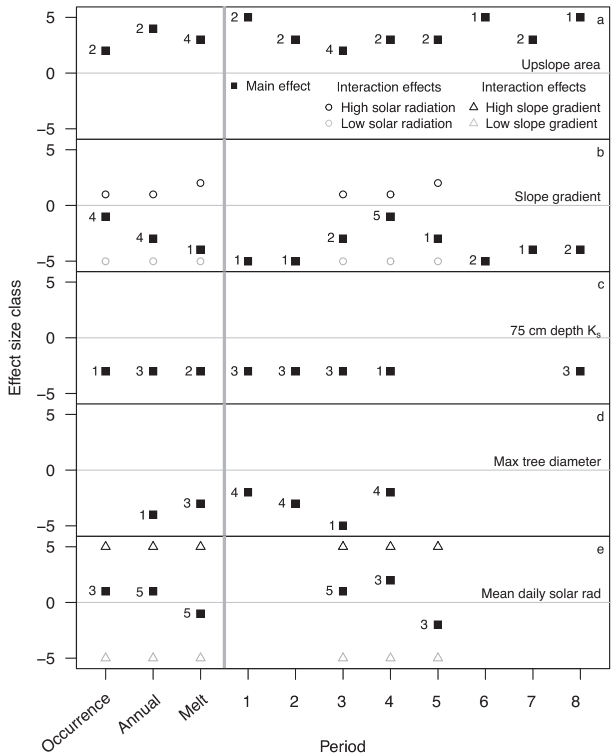

Fig. 5. Effect size class (effect size for each class: 1: 1–5, 2: 5–10, 3: 10–50, 4: 50–100, 5: > 100), direction of effect (positive or negative), and effect rank (indicated to the left of each point) for the predictor variables in the logistic regression models. Effect sizes were calculated by taking the exponential of the product of the coefficient and the range in the data between the 25th and 75th percentile values for each respective predictor variable. Interaction terms were ignored for calculating the main effects. For calculating the interaction effects, relevant interaction predictor variables were held at their respective minimum or maximum values.

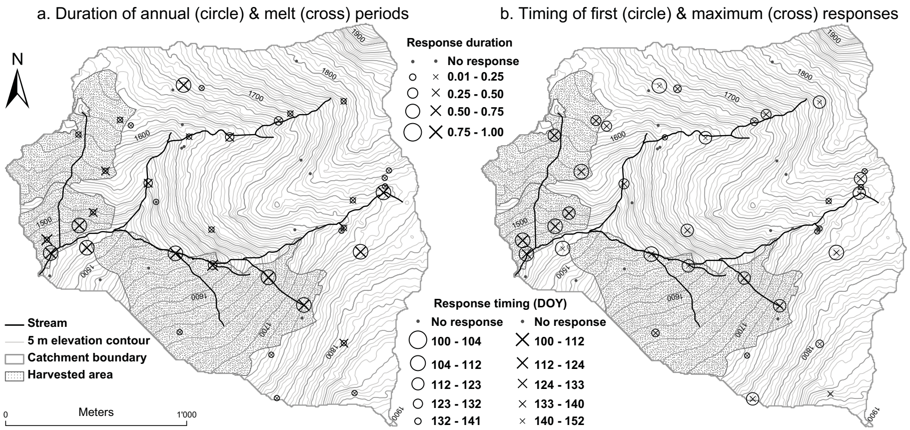

Fig. 6. Groundwater response duration (as a portion of the total duration of response in the period) at the hillslope sites for the annual and spring melt periods **(a)** and groundwater response timing (day of the year, DOY) at the hillslope sites for the first and maximum responses **(b)**. The timing of each period is indicated in Fig. 2.

HESSD
10, 2549–2600, 2013

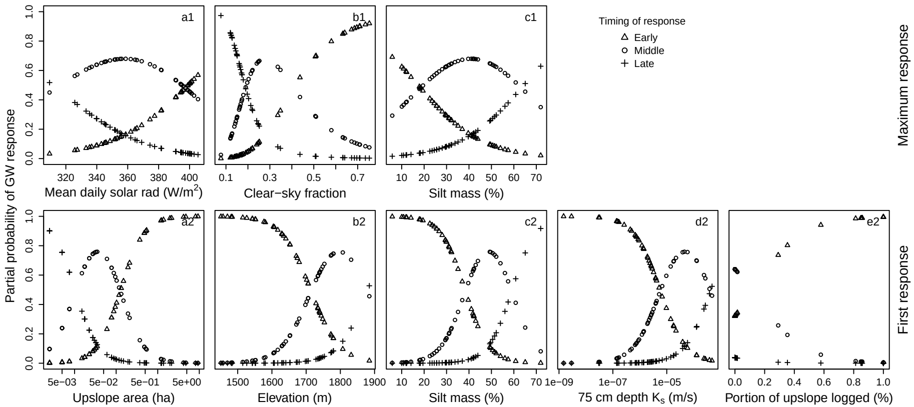

Fig. 7. Partial probability of groundwater response for each variable in the respective logistic regression models (indicated on the far right side of each row) predicting the timing of maximum response and the timing of first response. The timing of response (early, middle, or late in the spring melt) with the highest partial probability at any corresponding value of a predictor variable is the most likely outcome.

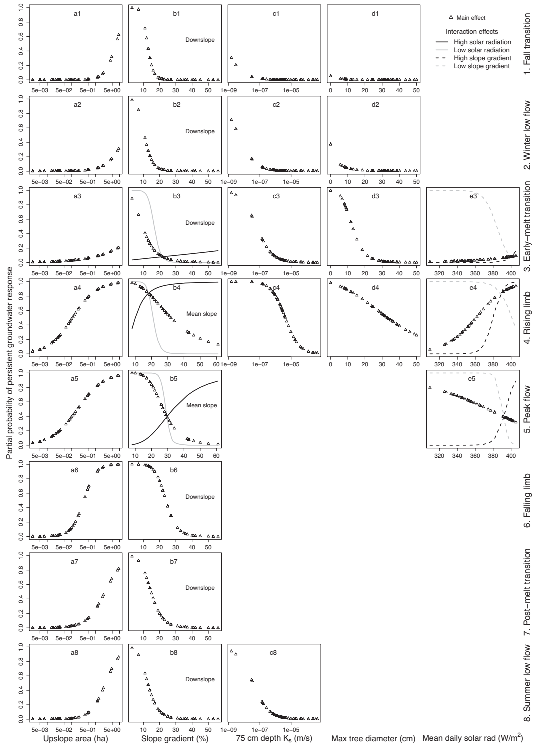

Fig. 8. Partial probability of groundwater response for each variable in the respective logistic regression models. For slope gradient, mean gradient versus downslope gradient is indicated. Response periods are indicated on the far right side of each row. Response variables for all rows are the persistence of groundwater response. For calculating the partial probabilities, all other predictor variables were held at their respective mean values except any relevant interaction predictor variables, which were held at their respective minimum or maximum values.

HESSD
10, 2549–2600, 2013

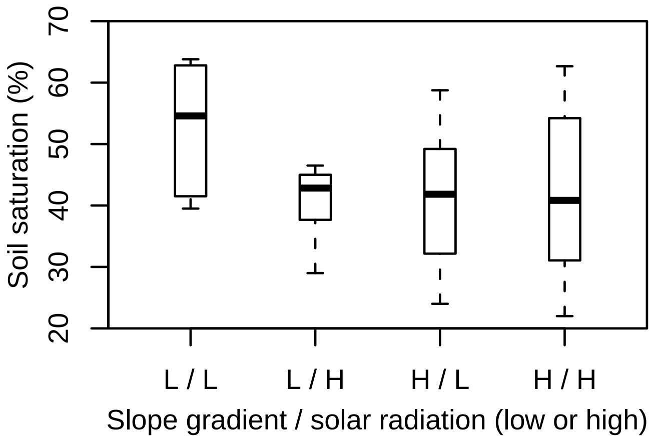

Fig. 9. Boxplots of soil saturation (mean of 10–40 cm soil depth) on April 6–8, 2008, combining sites of low or high mean slope gradient (i.e. less than or greater than the mean gradient) with sites of low or high spring melt potential solar radiation (i.e. less than or greater than the 25th or 75th percentile radiation, respectively) throughout the snow-free season.

HESSD
10, 2549–2600, 2013

Runoff dynamics in a snowmelt catchment

R. S. Smith et al.

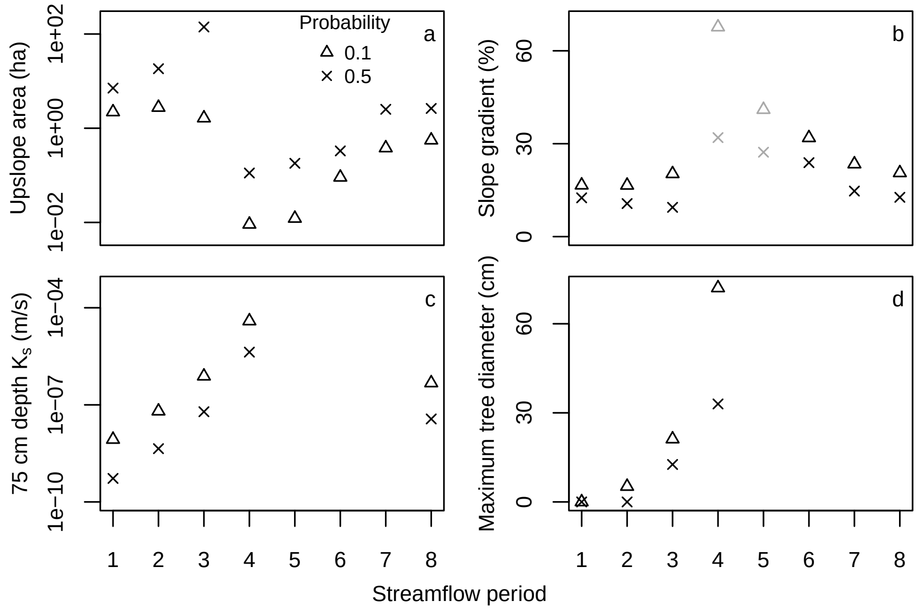

Fig. 10. Variation in the predicted values of **(a)** upslope drainage area, **(b)** slope gradient (downslope gradient in black, mean slope gradient in gray), **(c)** deep soil K_s, and **(d)** maximum tree diameter for the 10 % and 50 % partial probabilities of persistent groundwater responses. For calculating the partial probabilities, all other predictor variables were held at their respective mean (geometric mean for K_s) values.